ZIBELINE INTERNATIONAL PUBLISHING

Journal of Mechanical Engineering Research and Developments (JMERD)

DOI : http://doi.org/10.26480/jmerd.03.2018.27.31

ISSN: 1024-1752

CODEN : JERDFO

CrossMark

MICROSTRUCTURES AND ELEMENTS DISTRIBUTION IN THE TRANSITION ZONE OF CARBON STEEL AND STAINLESS STEEL WELDS

T.Nhung Le[1,2], M.Khanh Pham[2], A.Tuan Hoang[3,4], D.Nam Nguyen[1]

[1]Vietnam Maritime University, Vietnam
[2]Hanoi University of Science and Technology
[3]Ho Chi Minh city University of Transport
[4]The Central Transport College VI, Vietnam
**Corresponding Author Email: lenhung.vl.hh@gmail.com*

ARTICLE DETAILS

Article History:

Received 23 May 2018
Accepted 24 September 2018
Available online 27 September 2018

ABSTRACT

The change of microstructures and elements distribution around the carbon fusion line in carbon steel and stainless steel welds were investigated by means of optical microcopy (OM), scanning electron microscopy (SEM) and energy dispersive spectroscopy (EDS). The chemical composition profiles of the interface lay varied continuously from the base metal to the weld zone of 80μm width. This study showed that the microstructures and properties of this zone depended on local composition and cooling rate. Fully Martensitic layer with 5μm of width was observed along the fusion line. Then, a fully Austenitic zone spreads over 20μm and a two-phase γ + δ microstructure typical of a stainless steel was documented from the fusion line to the weld metal. The hardness value of Martensitic is the highest and recording 243 HV. The results may be used to overcome the limitations of the weld structure zone between carbon steel and stainless steel for application in the shipbuilding industry.

KEYWORDS

Carbon steel, stainless steel, dissimilar metal welds, element distribution, microstructure.

1. INTRODUCTION

Dissimilar metal welding of carbon steel to stainless steel presents a number of metallurgical and engineering challenges. Because of the difference composition between the base metal and the filler, two dissimilar metals are welded together lead to welding transition zone where have the formation of different microstructures and properties from the adjacent regions.

The chemical composition profiles varied continuously from the base metal to weld metal [1,2]. Fluid motion and solute transport are the phenomena usually mentioned to explain composition evolution in dissimilar welds [3]. But solidification segregations have to be used to completely describe the complex shape of the profile in the transition layer. In addition, Martensite was reported to form at the interface [4,5]. The microstructures range normally from fully Martensite to fully Austenite or may exhibit mixtures of Austenite, Ferrite, and Martensite [6]. The Martensitic layer width with high hardness varied significantly because of changing the local compositional gradient and cooling rate [7]. Most of the studies have based their phase identification on dilution calculations and the Schaeffler diagram only, while some authors have reported Martensitic laths observed by means of Transmission Electron Microscopy (TEM) [8]. In brief two main points should be noticed

(i) The relation between the distribution of alloy elements in the transition zone causes to change of microstructures and properties of weldment;

(ii) The high hardness and brittleness of the Martensitic layer along the fusion line can reduce mechanical properties.

This paper presents an investigation of the element distribution as well as microstructural changes in the carbon transition zone of dissimilar welds between carbon steel and stainless steel [9,10]. Martensitic transformation can be discussed by Martensitic start temperature, local chemical composition gradient, rapid cooling rate [11]. In facts, Martensitic start temperature can be predicted by following the empirical formula:

For the carbon steel (with no alloying elements whose content is higher than 5%) [12,13]:

Ms (0C) = 561 – 474%C – 33%Mn – 17%Cr – 17%Ni – 21%Mo
For the stainless steel [14]:

Ms (0C) = 502 – 810%C – 13%Mn – 12%Cr – 30%Ni – 6%Mo
In addition, a cooling rate that caused of Martensitic transformation can be determined by CCT diagram shown in Figure 1.

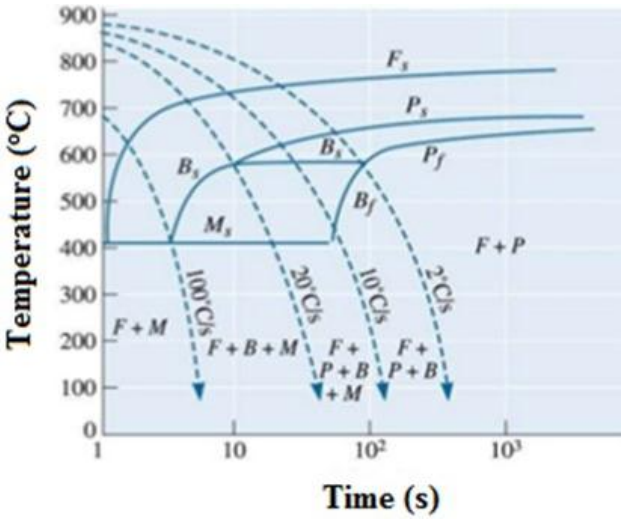

Figure 1: CCT diagram of 0.2%C [9]

The cooling rate is below 100°C/s lead to Austenitic to Martensitic transformation [15]. Figure 2 is the isoplethal section of the phase diagram for the carbon steel, the composition of the base metal being identified by an arrow. This was used to explain the microstructure evolution of fusion zone next to the fusion line.

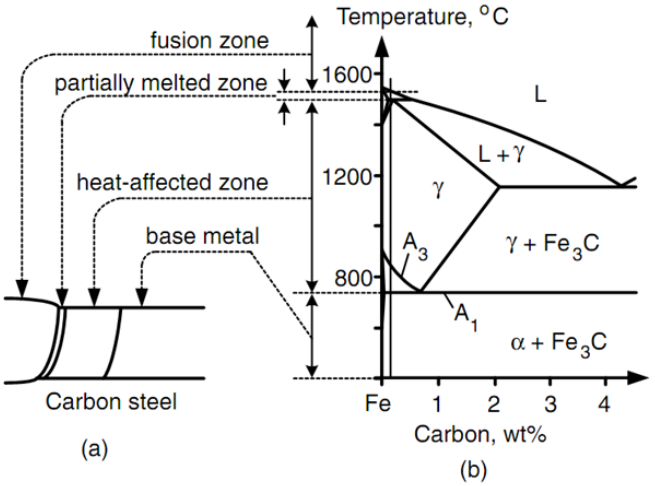

Figure 2: The microstructure of the weld

The phase diagram of Fe - C and the CCT is used in determining the phases and changes occurring during the heating of carbon steel. However, it can still be used in the welding process with the following points: First, the temperature reached during welding at the zone of thermal effect (HAZ) can reach 1500°C, while the maximum temperature of the heating process is 900°C, not much higher than the critical temperature A3 for the transformation austenite process. Secondly, the cooling rate of the welding process is very high, the time required for the austenite to remain in the austenite state is very short, while for the heating process, the heating rate is much lower and the retention time A3 longer [16]. Temperatures A1 and A3 during heating are often referred to as Ac1 and Ac2. The reason that the temperature Ac1, Ac3 when heated higher than the temperature in equilibrium A1 and A3 because when the heating rate increases, the critical temperature also increases.

According to the theory of dynamics, the phase transformation requires the difference in concentration of substances and time to occur diffusion process. Therefore, during the welding process, due to the very fast heating rate, the phase transformation may not occur at temperatures of A1 and A3 at higher temperatures than Ac1 and Ac3. For steel, there is a mass of carbide-forming elements (V, W, Cr, Ti, Mo) because the diffusion rate of these elements is lower than that of carbon, so it impedes the diffusion of carbon. During welding process, due to the combination of high heating speed and shortening time on Ac3, so the austenite will be uneven. As a consequence, HAZ's microscopic rigidity changes over a fairly wide range. In addition, the area near the grain boundary is growing rapidly due to the high temperature and the retention time on Ac3 for quite a long time, so the mechanical properties of this region are very low.

2. SEXPERIMENTAL SETUP

The rectangular specimens of carbon steel and 304 stainless steel with a size of 275 x 85 x 3 mm were welded together using shielded metal arc welding (SMAW). Filler E309L – 16 with 3.2 mm diameter was utilized. The chemical composition of base metals and filler are shown in Table 1. The welding parameters used in the experiment are presented in Table 2. Besides, a thermocouple was used to measure thermal cycle at the fusion line of weld that was used to determine the Martensitic start temperature and cooling rate (Figure 3).

Table 1: The chemical composition

Alloys	C (%)	Mn(%)	Si(%)	S(%)	P(%)	Cr(%)	Ni(%)	Mo(%)	V(%)
304 stainless steel	0.09	1.54	0.49	0.005	0.005	18.3	7.56	0.13	0.11
Carbon steel	0.18	0.62	0.02	0.04	0.05	0.02	0.08	0.005	0.01
Filler E309L - 16	0.03	1.34	0.71	0.005	0.003	23.7	12.6	-	-

Table 2: The welding parameters of the single-pass welding

Parameters	I (A)	U (V)	V (mm/min)	Preheat (°C)
Values	80	25	100	30

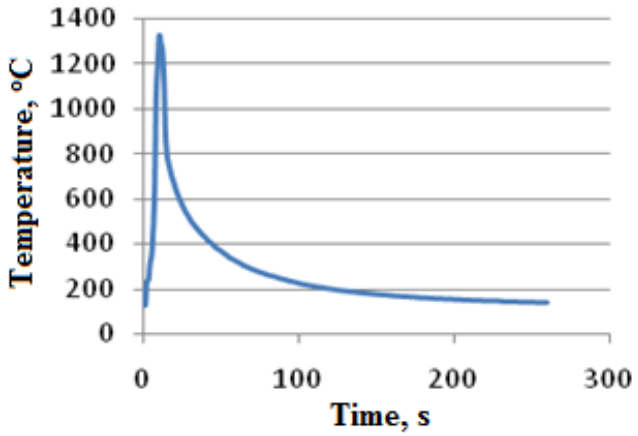

Figure 3: Welding preparation

After welding, some specimens were machined and prepared for metallographic tests. Because there was a remarkable difference in the corrosion behavior of different zones in the welded joints, two etchants were used to distinguish and display clearly microstructures and characteristics in each zone:

1) 3% of HNO_3 for carbon steel;

2) 5g of $FeCl_3$ + 15cm³ of HCl and 50 cm³ of H_2O, hydrochloric acid and alcohol solution for stainless steel and weld metal.

The microstructure was observed by OMLEICA MDS4000M, and the hardness values were measured by hardness tester ARK600. EDS line was used to measure the concentration profiles of alloy elements across joints by JSM-5410LV.

3. RESULTS AND DISCUSSIONS

3.1 Elements distribution in the transition zone

In this experiment, EDS line on a transverse section of the weld was used to indicate the distribution of elements around the carbon fusion line that is plotted in Figure 4 for Fe, Cr, Ni, Mn. The profiles can be divided into three distinct zones: a flat plateau of the weld metal which remained after solidification; then the transition zone which composition gradients take place with 80µm width; and finally a flat part of base metal. Figure 5 indicates elements composition in the weld zone, the base metal and at the fusion line.

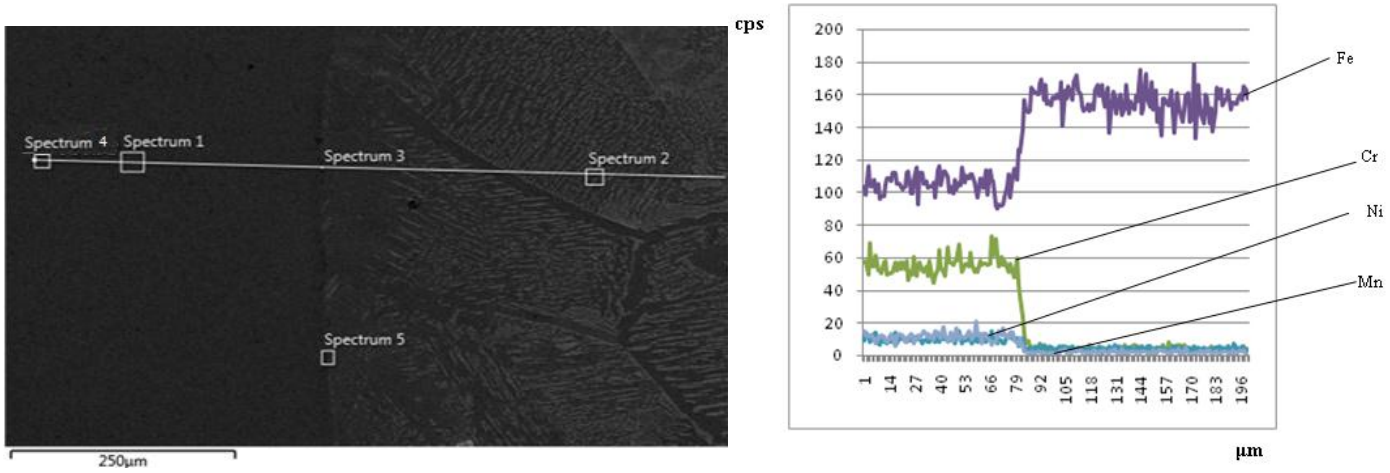

Figure 4: Elements distribution profiles in the transition zone

The results of the EDS analysis show that the content of Cr, Ni has shifted from the welding zone to the base metal. This shows the diffusion of the alloying elements from the welding zone to the base metal. In addition, the results of the EDS point analysis showed that the increased carbon content demonstrated the potential for carbide phase formation in the welding zone. The appearance of carbides of Cr; Fe and complex carbides if dispersed evenly increase the mechanical properties of the welding zone.

Spectrum 1: There is diffusion of carbon from the base metals to the welding zone; Because the carbon content in the center of the welding zone is low. However, the carbon content of up to 3% can be seen here as the formation of carbides of Cr or complex carbides.

Spectrum 2: Disappearance of Cr indicates that after welding there is no time for Cr to diffuse into the HAZ. The results of the analysis show that only Fe and C appear so that they can form carbides of Fe_3C.

Spectrum 5: Analyzing the boundary between HAZ zone and the welding zone showed that the content of Cr and Ni increases slightly compared to base metals (%Cr = 3.8% and %Ni = 1.3%). This can be explained by the diffusion of elements from the welding zone to the base metal boundary. There is a mixture of elements of the two alloying elements; this leads to an increase of the alloying elements on the boundary between the base metal and the welding zone.

The high carbon content here also makes it easier to form carbide at the grain boundary (here it is easy to form carbide of Chromium). It is the presence of carbides that will increase the microhardness in this region. Furthermore, with the carbide in the grain boundary, if not dispersed, it also causes damage to the welding.

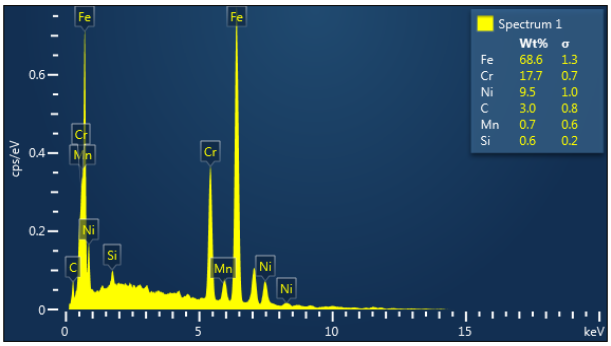

(a)

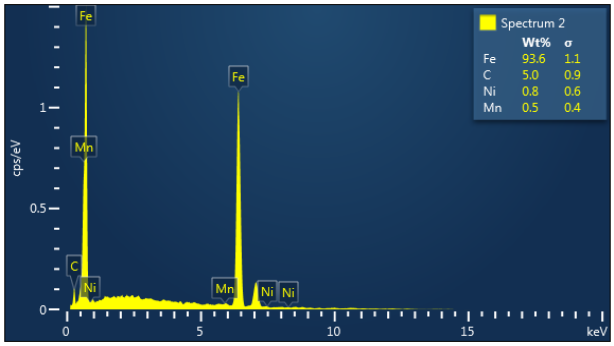

(b)

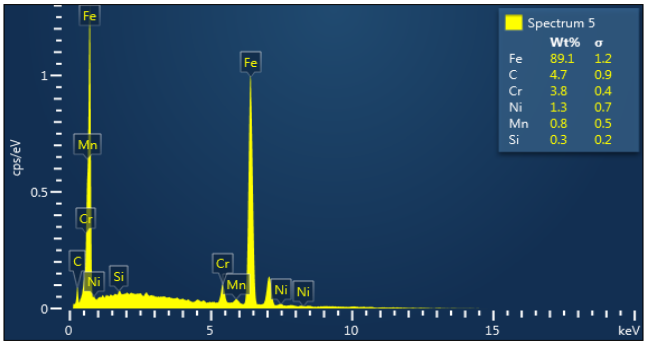

(c)

Figure 5: Elements composition, (a) Weld zone, (b) Base metal, (c) At the fusion line

3.2 Microstructures in the transition zone

The interface between heat affected zone of carbon steel and weld metal was distinguished clearly. However, microstructures can be observed at the fusion boundary of the welds. Various forms of microstructures are shown in Figure 6, including island (Figure 6b), beach (Figure 6c, e) or peninsula (Figure 6d). The filler metal in arc welding is different in composition from the base metal cause microstructures along the fusion line. The microstructures found at the fusion line shows the diffusion between the center of the weld and the base metal. This will help to ensure the bonding between the solder and the base metal, thus increasing the mechanical strength of the weld. The microstructures that measured from the boundary layer toward the base metal were fully Martensitic (black layer along the fusion line) to fully austenitic (white layer) then exhibit mixtures of austenite and ferrite (Figure 7).

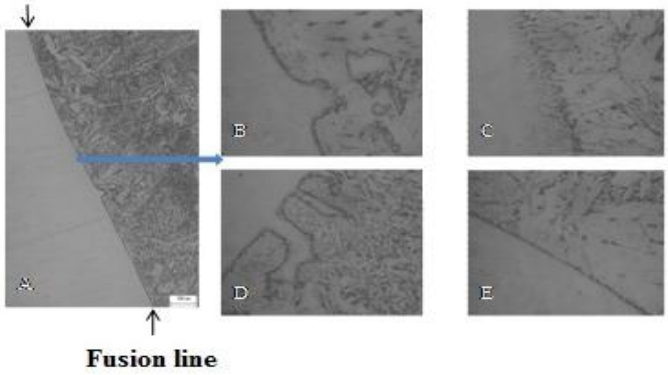

Figure 6: (A) Microstructures at the fusion line, (B) island, (C, E) beach, (D) peninsula

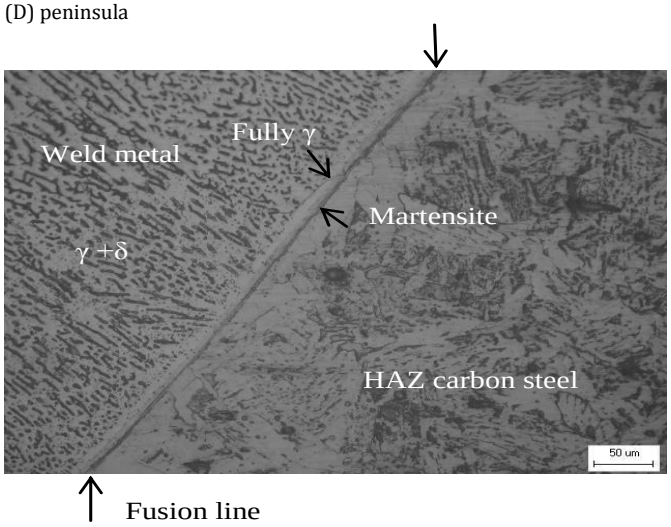

Figure 7: Microstructures in the transition zone

The observation of martensitic layer along the fusion line can be explained by the local composition and cooling rate. The rapid cooling rate was measured base on thermal cycle (Table 3) is 1100C/s from melted temperature to 800^0C or 240C/s during (800 – 500)^{0}C, higher than critical value was determined from CCT diagram. Besides, the local composition of the matrix in the martensitic layer has been reported by around 4%Cr and 2%Ni. A fully austenitic zone spreads over 20µm, then a two-phase γ + δ microstructure typical of a stainless steel. The fully austenitic zone in the weld metal can be explained by thermodynamic (Figure 2). This suggests that the high heating rate encountered during the welding process did not allow the nucleation of the δ–phase as equilibrium condition; therefore only austenitic grains would be directly in contact with the molten liquid, which makes easier their growth upon cooling. Moreover, the local composition with low alloy elements values in this zone can be added to explain the disappearance of δ. With optical microcopy analysis results show that in the fusion line there is the Martensite. This is in line with the results of the above EDS analysis (elevated C content in the bordering area and base metals).

3.3 Hardness values in the transition zone

Table 4 presents hardness values in the transition zone. The highest hardness was documented at the fusion boundary where fully martensite layer was formed. Although martensite layer has a high hardness and brittleness, this zone was not the weakest in the weld. The result of the tensile test shows that HAZ of carbon steel was usually broken. Tensile value presents in Table 5. Figure 9 and Figure 10 show the microstructure of the fracture surface.

Table 4: Hardness values

Positions	Fusion line		Weld metal	Carbon steel	
Distance from fusion line (µm)	0	100	200	100	200
Hardness (HV)	243	173	160	146	134

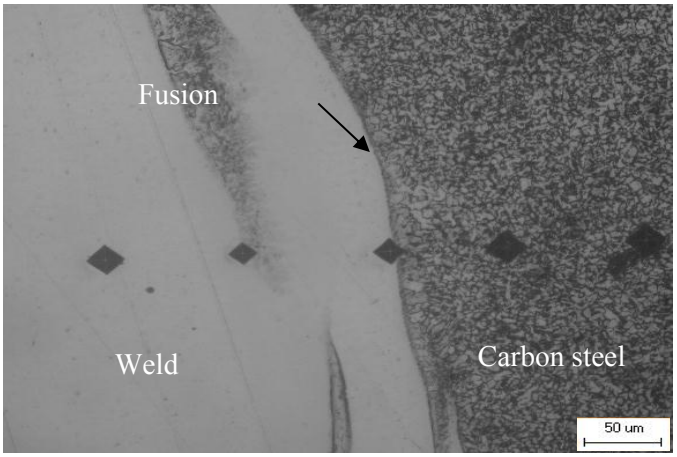

Figure 8: Microstructures of hardness test

Table 5: Tensile values

Tensile strength (N/mm^2)	Break position
442.8	Base metal

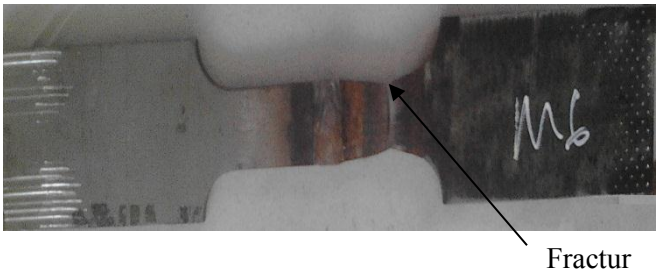

Figure 9: Tensile test sample

Analysis of the test specimen showed that the destruction site of the sample was in the HAZ. In this area, due to the stresses and grain size in this area, it is easy to damage the sample. Therefore, a treatment regime is needed to increase the strength of the weld in this area. These are also issues that will be addressed in subsequent studies.

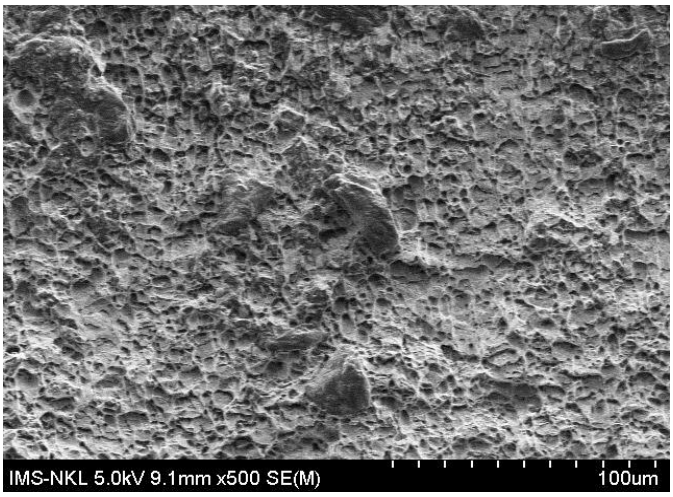

Figure 10: Tensile test sample

4. CONCLUSIONS

In this work, the microstructures and alloy distribution of dissimilar weld between carbon steel and stainless steel in the transition zone were investigated. From this study, the following conclusions can be drawn:

• The elements composition profiles in the transition zone varied continuously from the base metal to the weld metal with 80μm width. The difference of local composition caused the change of microstructures and properties of this zone.

• Microstructures can be observed along the fusion line with different shapes such as island, beach or peninsula.

• Fully Martensite layer with 5μm width was formed along the fusion line. The hardness value of this zone is highest by 243 HV. A fully austenitic zone spreads over 20μm, then a two phases of γ + δ microstructure typical of a stainless steel.

REFERENCES

[1] Muthupandi, V., Srinivasan, P.B., Seshadri, S.K., Sundaresan, S. 2003. Effect of weld metal chemistry and heat input on the structure and properties of duplex stainless steel welds. Materials Science and Engineering: A, 358 (1–2), 9–16.

[2] Nishiyama, Z. 2012. Martensitic transformation. Elsevier.

[3] Pham, X.D., Hoang, A.T., Nguyen, D.N., Le, V.V. 2017. Effect of Factors on the Hydrogen Composition in the Carburizing Process. International Journal of Applied Engineering Research, 12 (19), 8238–8244.

[4] Pham, M.K., Nguyen, D.N., Hoang, A.T. 2018. Influence of Vanadium Content on the Microstructure and Mechanical Properties of High-Manganese Steel. International Journal of Mechanical & Mechatronics Engineering IJMME-IJENS, 18 (2), 121-127.

[5] Shah, K., ul Haq, I., Khan, A., Shah, S.A., Khan, M., Pinkerton, A.J. 2014. Parametric study of development of Inconel-steel functionally graded materials by laser direct metal deposition. Materials and Design, 54, 531–538.

[6] Speer, J., Matlock, D.K., De Cooman, B.C., Schroth, J.G. 2003. Carbon partitioning into austenite after martensite transformation. Acta Materialia, 51 (9), 2611–2622.

[7] Kaufmann, S. 2011. Modulated martensite: why it forms and why it deforms easily. New Journal of Physics, 13 (5), 53029.

[8] Avramovic-Cingara, G., Ososkov, Y., Jain, M.K., Wilkinson, D.S. 2009. Effect of martensite distribution on damage behaviour in DP600 dual phase steels. Materials Science and Engineering: A, 516 (1–2), 7–16.

[9] de Andrés, C.G., Caballero, F.G., Capdevila, C., Alvarez, L.F. 2002. Application of dilatometric analysis to the study of solid–solid phase transformations in steels. Materials Characterization, 48 (1), 101–111.

[10] Howell, P.R., Bee, J.V., Honeycombe, R.W.K. 1979. The crystallography of the austenite-ferrite/carbide transformation in Fe– Cr– C alloys. Metallurgical Transactions A, 10 (9), 1213–1222.

[11] Bhole, S.D., Nemade, J.B., Collins, L., Liu, C. 2006. Effect of nickel and molybdenum additions on weld metal toughness in a submerged arc welded HSLA line-pipe steel. Journal of Materials Processing Technology, 173 (1), 92–100.

[12] Yang, H.S., Bhadeshia, H. 2009. Austenite grain size and the martensite-start temperature. Scripta Materialia, 60 (7), 493–495.

[13] Leem, D.S., Lee, Y.D., Jun, J.H., Choi, C.S. 2001. Amount of retained austenite at room temperature after reverse transformation of martensite to austenite in an Fe–13% Cr–7% Ni–3% Si martensitic stainless steel. Scripta Materialia, 45 (7), 767–772.

[14] Byun, T.S., Hashimoto, N., Farrell, K. 2004. Temperature dependence of strain hardening and plastic instability behaviors in austenitic stainless steels. Acta Materialia, 52 (13), 3889–3899.

[15] Azouggagh, M., Nebgui, A., Oussouaddi, Q., Haterbouch, M., Zeghloul, A. 2017. Study of Fatigue Crack Propagation in the Austenitic Stainless Steel 304L. International Journal of Mechanical and Mechatronics Engineering, 17 (5), 114–120.

[16] Nhung, L.T., Khanh, P.M., Hai, L.M., Nam, N.D. 2017. The relationship between continuous cooling rate and microstructure in the heat affected zone (HAZ) of the dissimilar weld between carbon steel and austenitic stainless steel. Acta Metallurgica Slovaca, 23 (4), 363-370.